THE JOURNAL OF PHYSICAL CHEMISTRY B

ARTICLE

pubs.acs.org/JPCB

Femtosecond UV Studies of the Electronic Relaxation Processes in Cytochrome *c*

Olivier Bräm, Cristina Consani, Andrea Cannizzo,[†] and Majed Chergui*

Laboratoire de Spectroscopie Ultrarapide, ISIC, Ecole Polytechnique Fédérale de Lausanne, CH-1015, Switzerland

Supporting Information

ABSTRACT: We report on an experimental study with UV and visible ultrafast time-gated emission and transient absorption of the early photodynamics of horse heart Cytochrome *c* in both ferric and ferrous redox states. A clear separation in time and energy of tryptophan and haem emission is observed. Excitation of the haem via resonant energy transfer from the tryptophan residue is observed in the subsequent haem electronic relaxation. Different Trp−haem energy transfer time constants of the ferrous and ferric forms are obtained. An almost instantaneous relaxation to the lowest singlet excited state (corresponding to the so-called Q band) characterizes the earliest electronic dynamics of the haem, independent of excitation energy, while dark intermediate states govern the ground-state recovery. The information gathered in these two experiments and in the literature allows us to propose a simple scheme for the electronic relaxation leading to ligand dissociation.

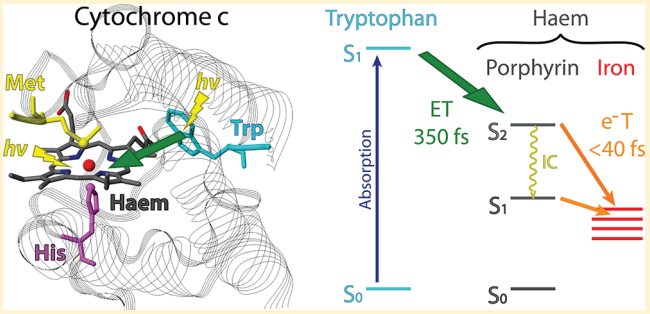

INTRODUCTION

The mechanism of ligand release and rebinding in hemoglobin and myoglobin has been extensively studied by ultrafast pump−probe spectroscopy in which an impulsive photoexcitation dissociates the ligand, while the evolution of the system is followed using a second time delayed pulse.[1−9] However, the details of the electronic structure changes that are responsible for the photodissociation are still not elucidated. In particular, from which electronic excited state does the bond breaking occur and how fast it is populated are still unanswered questions. To address these issues, here we focus on the photoinduced dynamics of horse heart Cytochrome *c* (hh Cyt *c*, Cyt *c* in the following) using ultrafast spectroscopy with excitation and detection in the UV, in the region where the tryptophan residue absorbs and fluoresces. Cyt *c* is a relatively small and highly soluble hemoprotein, loosely associated with the inner membrane and involved in the electron transport chain of mitochondria.[10,11] The Cyt *c* active site consists of a 6-coordinated iron porphyrin capable of undergoing oxidation and reduction. Histidine (H18) and methionine (Met80) residues constitute the biaxially ligated side chains of its haem and are of particular relevance to its stability and functionality.[4] Moreover, both ferric and ferrous redox states play important physiological roles. The photodissociation of its Met80 axial ligand upon visible excitation[12,13] makes Cyt *c* a useful system to study the geminate ligand photodissociation−recombination cycle. Furthermore, in hemoproteins, the photoexcited Trp residue is known to undergo Förster−Dexter resonance energy transfer to the haem group, whose efficiency depends on the distance and relative orientation of the Trp−haem pair.[14,15] For this reason, it has been extensively used to study protein folding through emission quantum yield (QY) measurements.[16,17] Cyt *c* contains only one tryptophan residue, very close to the haem group (∼9 Å), and known to undergo very efficient energy transfer to it.[18] Such Trp fluorescence quenching has already been reported in other hemoproteins by Zhong and co-workers using the up-conversion technique.[19−21]

The primary photoprocesses of ferrous Cyt *c*, after photodissociation, have already been investigated by femtosecond transient absorption exciting the cofactor within the so-called Soret or Q bands (400−420 nm and 500−560 nm, respectively) and probing it in the visible range.[12,13] The derived picture is the photolysis of the Met axial ligand in tens of femtosecond followed by its geminate recombination, accompanied by internal vibrational redistribution (IVR) and cooling dynamics. In the past decade, several groups have strongly suggested that the impulsive photodissociation occurs via an electron transfer from the porphyrin macrocycle to the antibonding axial d-orbital of the metal.[8,22−24] The subsequent ligand-cleavage brings the haem from a 6- to a 5-coordinated high-spin state, and causes a doming of the porphyrin plane.[12,13] While the Met80 photodissociates in the ferrous form of Cyt *c*, only cooling dynamics occurs in the ferric form, with no signature of ligand photolysis.

In a parallel article, we reported the vibrational energy redistribution and heat dissipation in Cyt *c*.[25] Excitation within the Q band, Soret band, and at 290 nm, where both tryptophan and haem absorb, were achieved to explore the relaxation pathways

Received: August 8, 2011
Revised: October 12, 2011
Published: October 17, 2011

of higher energy haem states, but also of the tryptophan residue. Moreover, these different excitations would induce an increase of the haem temperature by 300, 400, and 550 K, respectively, allowing us to study the role of the excess vibrational energy on the observed dynamics.[26] The data showed relaxation and cooling processes with different time scales in the two redox states, but independent of the excess of energy deposited in the haem. Here, we complement this study by the first fluorescence up-conversion study of Cyt *c*, with excitation and probing in the visible as well as in the UV,[27,28] accessing both haem and Trp excited states. Along with broadband transient absorption experiments, this work reveals the subpicosecond electronic relaxation of ferric and ferrous Cyt *c*, covering the entire photocycle, until the recovery of the electronic ground state.

MATERIALS AND METHODS

Sample Preparation. Horse heart Cyt *c* was purchased from Sigma Aldrich. The solution was prepared by dissolving 140 mg of Cyt *c* in a 30 mL of buffer at pH = 7 (deionized water with KH_2PO_4 + NaOH 10 mM), giving a concentration of 0.39 mM, and a corresponding optical density of 0.2 at 286 nm in the 0.2 mm-thick quartz flow cell used for the experiment. No oxidant was added to the solution of ferric Cyt *c*. To obtain the ferrous form of Cyt *c*, the sample was previously reduced by addition of sodium dithionite $Na_2S_2O_4$ salt. The sample was then desalinated using a gel-filtration chromatography column.

Ultrafast Time-Gated Fluorescence Measurements. The ultrafast broadband UV fluorescence setup, based on the up-conversion scheme, has been previously described.[27,29,30] Briefly, the output of an 800 nm fs-regenerative amplifier system, operated at 130 kHz, is used to pump a vis-OPA generating 592 nm pulses. After frequency doubling, we obtain 286 nm pump pulses with a bandwidth of about 4 nm and a pulse width of about 70 fs. The excitation energy of 23 nJ/pulse was chosen so as to be in the linear regime of excitation such that only the Trp or the haem are excited per protein. The UV-excited emission from the sample is filtered with a 300 nm cutoff filter to remove the remaining excitation light, and then mixed in a 250 μm-thick BBO crystal with the 800 nm gate beam. The up-converted signal is detected with a CCD camera-equipped monochromator. To overcome the phase-matching condition at the sum frequency crystal, the latter is turned around the ordinary axis at each delay time to cover all of the phase-matching angles corresponding to the desired spectral range. Because we use a type I sum frequency process, our detection is intrinsically polarization selective such that a magic angle polarized detection scheme was achieved by placing a half-wave-plate in front of the UV beam before excitation. The temporal and spectral responses of 160 fs and 6 nm, respectively, were determined by a measurement of the Raman response from the solvent (data not shown). Data were spectrally corrected to account for the instrumental spectral response and the distortions due to partial reabsorption.

Ultrafast Transient Absorption Measurements. A detailed description of the transient absorption setup has been recently reported.[31] We use 288 nm pulses with a spectral width of ~5 nm and a temporal width of ~70 fs at a repetition rate of 1 kHz. The UV-excited sample is then probed with a 50 nm broad pulse, and three different scans are used to cover the 263−375 nm region. The time response of 130 fs is determined from cross-correlation measurement in pure water. Cross-phase modulation signals were dominant in the first 100s of fs, so that to avoid artifacts, the first

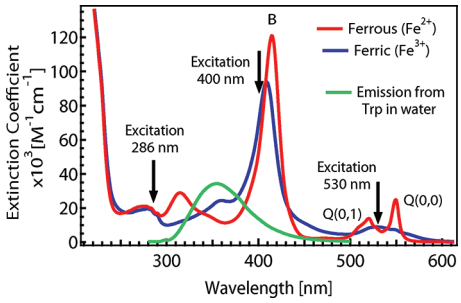

Figure 1. Absorption spectra of ferrous (red) and ferric (blue) Cyt *c* at pH 7. The excitation wavelengths are marked by arrows.

300 fs signals are not considered in the analysis. The 286−290 nm region is also removed due to scattering by the pump pulse.

Analysis. To reliably extract the spectral contribution of each time component, two different approaches were used: we performed a kinetic analysis (multiexponential fit) of the singular value decomposition (SVD) of each two-dimensional time-wavelength plot (see the Supporting Information). The results were verified by performing a global fitting procedure on kinetic traces taken across the total emission range in steps of 5 nm. We obtained the same decay associated spectra (DAS) and time constants from both analyses.

RESULTS

1. Steady-State Spectroscopy of Cytochrome *c*. Figure 1 shows the UV−vis steady-state absorption spectra of ferrous and ferric Cyt *c*. The haem group is responsible for the main features of these spectra with bands at 500−550 nm (Q band), 410−415 nm (B or Soret band), and 250−290 nm,[32−34] all due to porphyrin transitions. The 250−300 nm region contains the absorption band of Trp and slightly more to the blue, that of the four tyrosine residues. At the excitation wavelength of 286 nm, we estimate that ~25% of the absorption is due to the tryptophan, 65% due to the haem prosthetic group (the δ band[33]), and less than 10% due to the four tyrosine residues. This implies that upon excitation at this wavelength, for each excited Trp, we generate ~2.5 excited haem groups.

The UV fluorescence emission of Cyt *c* (300−450 nm) is expected to stem mainly from Trp residue.[4,18,35,36] However, Löwenich et al. reported a bimodal fluorescence, investigated through excitation-wavelength-dependent fluorescence spectroscopy.[37] They claimed that upon excitation at 280 nm and at pH 7, the iron porphyrin contributes about 80% and tryptophan about 20% to the total fluorescence. They fitted the stationary emission spectrum of Cyt *c* with two broad Gaussians, respectively, centered at 355 nm for the Trp contribution and 370 nm for the haem contribution.

2. Time-Resolved Fluorescence. *a. Results.* Figures 2a and 2b shows spectra at different time delays, selected from the time−wavelength plots of the emission of ferrous and ferric Cyt *c* under 286 nm excitation, shown in Figures S1a and S1b. In both forms, the emission is broad and spans the 300−500 nm region. It decays on a subpicosecond time scale, with a faster decay component in the 400−500 nm region, which is pulse-limited, as it disappears at the same time as the water Raman peak at 317 nm. Moreover, no rise of the emission can be observed over the whole spectral range. This result reveals that two different spectral contributions are present from $t = 0$ but they decay with different time constants. The slower

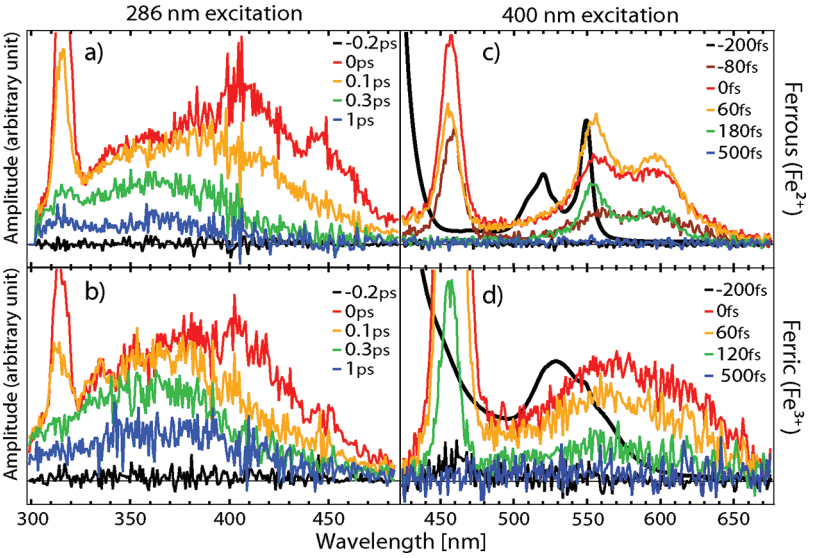

Figure 2. Representative sets of emission spectra at different time delays of ferrous and ferric Cyt *c* (top and bottom panels, respectively) upon 286 and 400 nm excitation (left and right panels, respectively). The strong peak at 317 and 463 nm for the UV and visible excitation corresponds to the instantaneous Raman signal from water. The corresponding static absorption spectra are the thick black traces in panels c and d.

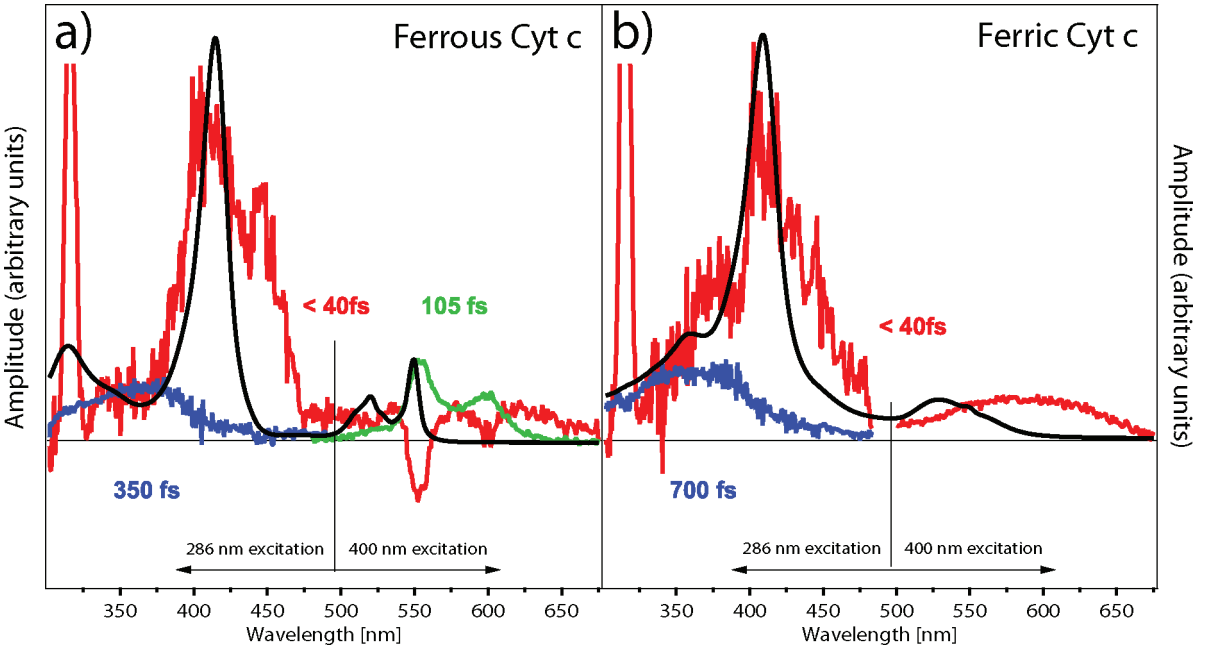

Figure 3. Decay associated spectra (DAS) resulting from the SVD analysis of time-resolved fluorescence of ferrous (a) and ferric (b) Cyt *c* of data of Figure 2. The corresponding stationary absorption spectra are shown as black traces.

decay observed in the blue region is faster in the ferrous as compared to the ferric form.

Moving to 400 nm excitation, Figures 2c and 2d present spectra at different delays, selected from the time-wavelength plot of the emission of ferrous and ferric Cyt *c* (Figure S1c and S1d). The two oxidation states show drastically different emission decays and spectral shapes. In the case of ferrous Cyt *c*, the emission spectra show a clear vibronic progression at all times, corresponding to the mirror image of the static absorption. The spectrum narrows down in tens of femtoseconds, as can be seen by comparing the time zero and the 60 fs spectra. The whole spectrum vanishes within 500 fs. In contrast, the emission spectrum of ferric Cyt *c* is broad, unstructured, and it disappears in less than 200 fs.

b. Spectral and Temporal Decomposition. Figure 3 shows the resulting DAS of ferrous and ferric Cyt *c* for both UV and visible excitation. For the UV (286 nm) excitation, a broad (300−450 nm) spectrum is centered around 370 nm, associated with a 350 and 700 fs decay time for ferrous and ferric Cyt *c*, respectively (blue traces), overlapping a narrower band around 370−470 nm associated with a <40 fs decay (red trace). As already observed in Figures 2c and 2d, under 400 nm excitation, the two

dx.doi.org/10.1021/jp207615u |*J. Phys. Chem. B* 2011, 115, 13723–13730

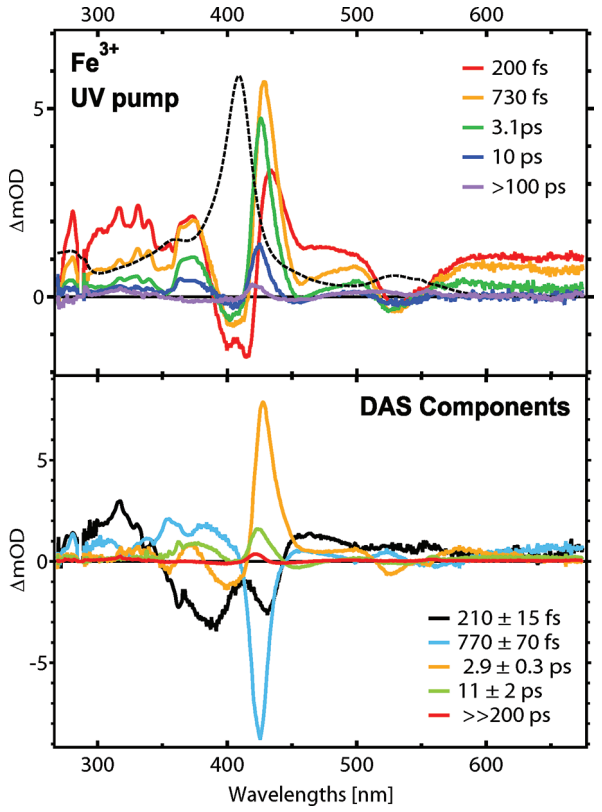

Figure 4. (top) A representative selection of transient absorption spectra at different delay times from ferric Cyt *c* under UV (288 nm) pump. The dashed line represents the ground-state absorption spectrum in arbitrary units. (bottom) DAS from analysis of femtosecond TA measurements of ferric Cyt *c* excited at 288 nm (top).

oxidation forms behave very differently. The ferric form shows only one broad positive spectral contribution associated with <40 fs decay (red trace). The ferrous form exhibits two structured DAS. The slowest clearly corresponds to the mirror image of the absorption (in black) and is associated with a 105 fs decay time (green trace). The fast contribution (red trace) is associated with a <40 fs time constant and looks like a positive, broad, and unstructured band with two sharp minima at positions corresponding to the peaks of the slow decay component (green trace). This component reflects the evolution from a broad and featureless emission to the structured one within our instrumental response and can be seen as a simultaneous rise and narrowing of the slower component.

3. Transient Absorption. The top panel of Figure 4 (Figure S2) shows a representative selection of TA spectra from ferric (ferrous) Cyt *c* under UV excitation.[25] We observe a complicated behavior where positive signals, due to excited-state absorption (ESA), are overlapping (negative) ground-state bleach signals, in addition to spectral evolution of some features. To disentangle these different contributions, we analyzed the SVD of the experimental data according to the procedure previously discussed. The outcome of this analysis is presented in the bottom panel of Figure 4 (Figure S2), where five DAS components are found, with relative time constants spanning from hundreds of femtosecond to tens of picosecond. For the present purposes we will focus only on the subpicosecond components, because the long cooling-related ones are discussed in ref 25. For each redox form and under both UV and visible excitation, we observe a 150−220 fs component with a similar spectrum over all of the investigated spectral range. On the basis of this strong invariance and an overall absorption character (except where the Soret band dominates), we assign it to ESA on the porphyrin macrocycle. It will be referred as the excited-state (ES) decay time τ_{ES} in the following. In the case of ferrous Cyt *c* upon visible excitation, this component contains contribution from a rise of the subsequent photoproduct signal. Under UV excitation, an additional component of 350 and 770 fs has been detected in the ferrous and ferric forms, respectively. This time constant is attributed to the decay of the Trp excited state (τ_{Trp}) as will become clear later. Table 1 summarizes the time constants obtained from the analysis of the transient absorption and fluorescence data.

DISCUSSION

The results reported here exhibit various relaxation processes of Trp and haem in Cyt *c*, which we now discuss for both redox forms.

1. Trp Emission. We assign the slowest component at 370 nm (τ_{Trp} in Table 1) to emission from the Trp, even if a more blue-shifted band could be expected for such a deeply protein-embedded Trp. Indeed, the inner protein environment is hydrophobic, and in such a medium the fluorescence from Trp is known to lie at shorter wavelengths than the bulk water steady-state fluorescence.[38,39] However, the spectrum is red-shifted (∼10−20 nm) with respect to that of aqueous Trp, indicating that the Trp residue is located in a relatively polar environment.[39] Note that because of the excitation cutoff filter on the blue side and of the spectral correction, for strong reabsorption on the red side, the maximum of the band is affected by a large uncertainty, possibly being as short as 350 nm but not more. This is still quite an impressive Stokes shift with respect to the Trp emission in water and the latter interpretation is valid. This emission does not show any spectral evolution, which would be a signature of solvation dynamics. The lack of environment response on this time scale points to its rigidity, but has also to do with the fact that the fast Trp de-excitation (350 and 700 fs) excludes any response at longer time scales. These Trp decay times are unusually short as compared to the fluorescence lifetime in bulk water (3 and 0.5 ns), but this is in full agreement with the UV-TA measurements showing 350 and a 770 fs components for the ferrous and ferric forms, respectively (lower panels of Figure 4 and Figure S2), unambiguously assigned to Trp excited-state absorption (ESA). Moreover, in the visible region, where only the haem contribution is expected, a rise of the subsequent haem absorption signal is observed on the same time scales only upon UV excitation.[25] This delayed haem population, also observed in its emission (see section 3), is concomitant with the Trp de-excitation and provides unambiguous evidence of a very efficient Trp-haem energy transfer, on the time scales of 350 and 700 fs. This is also in agreement with fluorescence QY measurements as a function of pH,[18,37] if we compare them to the radiative decay of ∼3 ns measured in aqueous solution.[40]

The different decay times in the ferrous and ferric forms speak for a less efficient energy transfer in the latter. As can be seen in Figure 1, the dependence of the energy transfer efficiency cannot be ascribed to spectral changes of the haem absorption: if one takes the stationary emission spectrum of aqueous Trp as a reference, the overlap integral in the ferric form is 15% larger than in the ferrous form.[18] Therefore, the less efficient energy transfer in the ferric form is ascribed to the different relative orientation

Table 1. Time Constants Obtained from Exponential Fits of the SVD of Transient Absorption and Fluorescence from Ferrous and Ferric Cyt *c* under 286 (288 for TA), 400, and 530 nm Excitation

		transient absorption[25]		fluorescence up-conversion		
oxidation form, excitation [nm]		τ_{ES} [fs]	τ_{Trp} [fs]	τ_{Trp} [fs]	τ_{Soret} [fs]	τ_{Q} [fs]
ferrous	286	155 ± 12	350 (fixed)	350 ± 20	<40	120 ± 40 [70%]
						340 ± 140 [30%]
	400				<40	105 ± 5
	530	160 ± 15				145 ± 5
ferric	286	210 ± 15	770 ± 70	690 ± 30	<40	<40
	400				<40	<40
	530	220 ± 20				<40

and distance between the Trp residue and the haem cofactor, as found by structure determination (PDB: 1HRC and 1OCD). In addition, visible circular dichroism spectroscopy concluded to a different orientation of the haem transition dipole moment in the two redox states.[41] The oxidation state[42] and the nature of the protein fold are known to have a non-negligible influence on the tertiary protein structure of the haem pocket region.[33] In addition, compressibility measurements of Cyt *c* have pointed out that the ferric form has a more open tertiary structure than the ferrous one.[43] These observations agree with the experimental time scales obtained here of a less efficient energy transfer in the ferric case.

2. Haem Emission. In the 370−500 nm region, the pulse-limited contribution (red curve of Figure 3) matches well the B absorption (Soret) band, and therefore we assign it to ultrafast emission from the S_2 state, responsible for the Soret band. It has to be noted here that the strong absorption of the Soret band of our sample (>1 OD) might strongly affect the shape of the emission in the 400−430 nm region. Indeed, as a general feature of porphyrins, the Soret emission is expected to have a very small Stokes shift,[9,44] as a result of a weak vibronic coupling and of the fact that porphyrins are apolar chromophores. These results are to our knowledge the first time-resolved emission from the Soret band of a hemoprotein. Our instrumental response (160 fs) was too long to resolve the decay time (τ_{Soret}) of the S_2 state, and we can just provide an upper value of 40 fs. The time zero reference of the Raman band of water shows that the rise time of this emission is within our time resolution. From the excitation (at 286 nm) to the Soret band (400 nm), 1.22 eV is instantaneously dissipated. Moreover, as discussed in the next paragraph, the haem undergoes internal conversion (IC) to lower electronic excited states within 40 fs. These measurements allow us to calculate the relative emission QY of the Trp and haem moieties and to compare our time-resolved measurements with steady-state studies. From the area of the Soret and the Trp absorption bands, we can indeed estimate a radiative rate for the Soret transition approximately 10 times greater than that of Trp (one can roughly estimate this ratio from the absorption amplitudes of 120 000 and 6000 cm^{-1} mol^{-1} for the Soret and Trp absorption, respectively, taking into account that the Trp band is twice wider than the Soret band). With lifetimes of 40 and 350 fs, respectively, we find that the emission quantum yield is the same for both the haem and the Trp moieties. Interestingly, Löwenich et al.[37] observed that upon excitation at 280 nm and at pH 7, the haem contributes about 80% and tryptophan about 20% to the total stationary fluorescence. This is not far from our aforementioned contributions of 72% and 28% of haem and Trp to the total absorption; therefore, a similar estimation for the QY is derived.

In the 500−700 nm region, the observed emission is basically a mirror image of the Q band absorption. This structured emission is initially broad and narrows down within its rise time of <40 fs, to finally decay with a time constant of ∼100 fs. The narrowing of the bands is way too fast to be explained by cooling and rather points to a weak and broad hot emission spectrum instantaneously present, evolving by IVR during the excitation pulse to a more intense, narrow vibronic progression that is the mirror image of the absorption spectrum (Figure 2c). It agrees with the sub-40 fs Soret band emission decay time, pointing to a pulse-limited $S_2 \rightarrow S_1$ internal conversion and IVR (internal vibrational redistribution). The rise of the Q band emission is also observed upon UV excitation as shown in Figure 5. The emission decays with a time constant changing from ∼150 to ∼100 fs depending on whether we excite within the Q or the Soret band. This observation suggests an acceleration of the S_1 fluorescence quenching by excess of vibrational energy. The time scale obtained here is in accordance with the S_1 lifetime of ∼0.2 ps estimated on the basis of QY measurements.[45]

Contrary to the ferrous state, the ferric form shows only one DAS in the 500−700 nm region, with a shape corresponding somewhat to the mirror image of the stationary absorption band (black trace), but broader and associated with a pulse-limited (<40 fs) decay time, as is the Soret emission (Figure 3b). This lifetime is also expected from QY measurements.[45] As in the ferrous form, the $S_2 \rightarrow S_1$ internal conversion is virtually instantaneous, but the subsequent S_1 state relaxation dramatically changes with oxidation state.

3. Delayed Haem Excitation. We tracked down the energy transfer contribution from the Trp to the haem by monitoring the S_1 emission decay at 600 nm exciting in the UV (286 nm), within the Soret and Q bands (400 and 520 nm), as reported in Figure 5. Here, the decay of the S_1 emission is integrated over the spectral width of the red-most band (600 ± 20 nm, Figure S1c). Indeed, we see that the kinetics observed under Soret and Q band excitations are well described by a single decay, while the UV excited emission shows a biphasic behavior. The fit parameters are reported in the last column of Table 1. Beside the ∼120 fs decay, the additional slower decay (∼340 fs) has amplitude that is 30% of the total signal, close to the 28% contribution of the Trp absorption. An identical effect is observed with the TA analysis where the rise of haem-related signals is observed with the same time constant as the Trp lifetime (Table 1).[25] These observations lead us to conclude that this signal stems from the portion of haem molecules indirectly excited via energy transfer from Trp.

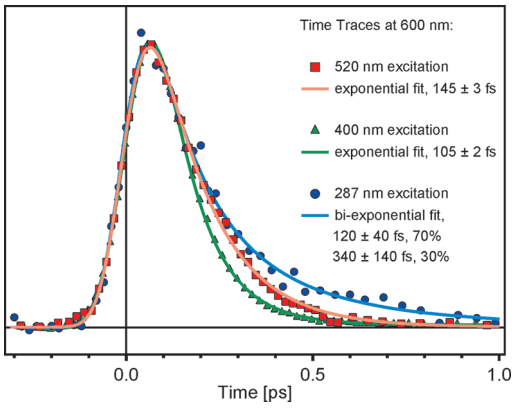

Figure 5. Normalized kinetic traces of the fluorescence of ferrous Cyt *c* in buffer solution pH 7 at 600 nm, under 286 nm (blue curve), 400 nm (green curve), and 520 nm (red) excitation.

This contribution should also show up in the Soret emission. As the haem emission is <40 fs while the Trp lifetime is at least 10 times longer, this signal decays with the longest time constant. In other words, it should appear in the DAS of the Trp emission. Indeed, the blue curves in Figures 3a and 3b shows a weak signal in the 400−480 nm region. This signal roughly matches the haem emission spectrum observed (red curve) when the latter is scaled by the excitation and time scale ratio (Figure S3).

4. Haem Electronic Relaxation. Under 400 nm excitation, an "instantaneous" population of the S_1 state is observed. Despite its rate, this is not the main depopulation channel from S_2, as only ∼15% of the excited molecules undergo $S_2 \rightarrow S_1$ IC in ferrous Cyt *c*.[45,46] The remaining 85% are believed to relax to the metal-centered states, triggering the ultrafast bond-cleavage.[13,24] Concerning the ferric form, branching ratios from higher states are unknown, because the very short excited-state lifetimes prevent static measurements. Because the ligand photodissociation QY is almost unitary (>80%)[13] whether we excite the Q, B, or δ band, the accepting metal-centered orbital is likely to be the empty antibonding d_{z^2}, because it is lower than all of the aforementioned porphyrin excited states and the lower metal-centered d_π orbital is fully occupied.[47]

Moving to the S_1 state (Q band), in both oxidation states it is populated upon 400 nm excitation from the S_2 state within our instrumental response, but it is depopulated in ∼100 fs in the ferrous form and <40 fs in the ferric one. These values are definitely shorter than the ESA lifetimes obtained from the TA measurements (150−220 fs), suggesting the presence of an intermediate state (a low-lying dark state or a hot ground state) in the latter that lengthens the recovery of the pristine porphyrin electronic ground state.

As previously discussed, only ∼15% of the molecules in the ferrous form relax to the S_1 state upon 400 nm excitation. They initially give rise to a very hot state, and the fluorescence appears within a few tens of femtosecond mirror-like with respect to the static absorption band. This points to the presence of a very effective IVR in damping the porphyrin high frequency modes, as was recently reported in metal−polypyridine complexes.[48] More important, it suggests that this emission stems from a 6-fold coordinated ferrous haem ($6cFe^{2+}$), rather than a 5-fold coordinated one ($5cFe^{2+}$). Indeed, the latter shows an unstructured broad absorption band, very similar to the 6-fold coordinated ferric haem ($6cFe^{3+}$).[12,13,25] Thus, we believe that the observed 100−150 fs decay time reflects an electron transfer from the porphyrin to an empty d-orbital of the metal (likely the d_{z^2}), and the subsequent ligand photolysis, under direct excitation of the Q band (inset of Figure S1c). It implies that the earliest TA dynamics describes also a $6cFe^{2+} \rightarrow 5cFe^{2+}$ conversion and not a porphyrin ESA only. This is almost 1 order of magnitude slower than the photolysis process upon 400 nm excitation[13] and than the generally assumed value compared to similar systems.[1,7,23] Noteworthy, when we consider the ferric form, the S_1 lifetime is pulse-limited regardless of the excitation, revealing an important role of the iron oxidation state and in particular of the d-orbital occupancy, involved in the porphyrin−iron bond.

Moving to UV excitation, Figures 3a and 3b shows that the pulse-limited signal matches well the expected S_2 emission in the overlap region 480−500 nm, confirming that the δ-state relaxes to S_2. Thanks to the tryptophan emission, which plays the role of an internal reference, we can estimate the QY of S_2 population by calculating the relative emission area at time zero integrated over the frequency domain in Figures 3a and 3b. This ratio is equal to the ratio of the initial number of emitters times the ratio of the radiative rates. The latter can easily be calculated as the ratio of the respective static absorption bands. The emission band ratio (S_2/Trp) is ∼4, while the Soret radiative rate is ∼7 times larger than the Trp one. As discussed in the Results, for each excited Trp, ∼2.5 haem groups are excited, yielding 20% of the excited hemes that end up in the S_2 state. Because the amplitude of the Soret band is distorted by a strong reabsorption, this value surely constitutes a lower limit, but suggests that the CT process also occurs from higher energy states of the haem.

Assuming that the relaxation pathway from S_2 does not depend dramatically on the excess vibrational energy deposited in the haem (direct excitation at 400 nm versus indirect excitation from higher states), molecules relaxing to S_2 will behave as the directly excited ones. Remarkably, regardless of the excited state, all of the lower electronic levels of the porphyrin are involved, with an instantaneous redistribution (population) among them. This is clear from Figure 5, where the rise of the signal at the lower transition is excitation wavelength independent.

To provide a unified description of these observations, we propose the photocycle summarized in Figure 6: in the ferrous form, upon excitation into the Q, B, or δ bands (step 1), the electron promoted to the e_g LUMO relaxes to the antibonding d_{z^2} metal-centered state (step 2, orange arrow), inducing ligand photodissociation. Thereafter, the pristine configuration is recovered by a back electron transfer (step 3) directly from the d_{z^2} orbital or indirectly from another d state (e.g., a $d_{xy} \rightarrow$ GS CT followed by a $d_{z^2} \rightarrow d_{xy}$ electron−hole recombination). The lifetime of the porphyrin ESA corresponds to the time of this back transfer.

The efficiency of the charge transfer triggering the ligand dissociation depends on the initially excited state. While it occurs within our instrumental response (<40 fs) from the S_2 state or from higher states, it is slower (100−150 fs) from the S_1 state. The shortening of the Q-band emission lifetime with the excitation energy (Table 1) suggests the presence of an energy barrier that needs to be overcome for the charge transfer to occur. The excess of vibrational energy (6000 or 15 000 cm^{-1}) provided by the 400 or 286 nm excitation improves significantly the CT process from S_1. Indeed, this large amount of energy is transformed into heat by IVR within our instrumental response, as witnessed by the pulse-limited rise of the Q-band emission.

The scheme of the photocycle shown in Figure S5 attempts a more unified description of the various processes at play, bearing

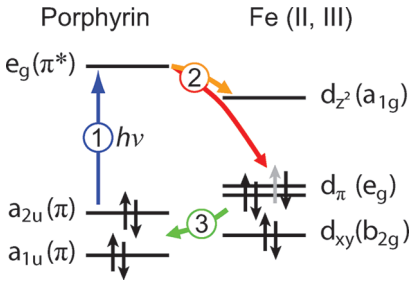

Figure 6. Photocycle of ferrous and ferric Cyt *c* haem, with the proposed relaxation pathways. Step 1: Light excitation to the e_g state (LUMO). Step 2: Charge transfer to the Fe empty d-orbitals. If the d_{z^2} metal center orbital is empty in both oxidation forms, the lower d orbitals are completely filled in the ferrous form, while in the ferric form the d_π one has one hole. The latter orbital constitutes a more efficient channel (red arrow) than the 100−150 fs IC to d_{z^2} (orange arrow). Step 3: Regardless of the relaxation channel, the final step to the haem ground state is an electron back transfer to the porphyrin macrocycle (relative energies and occupancy from ref 47).

in mind that the parabolae therein are only indicative, because we do not know the exact nature of the deformation. In the ferrous form, from the S_2 state the system experiences a branching with 86% of the molecules undergoing immediate internal conversion to the antibonding d_{z^2} metal orbital (channel A), inducing ligand photodissociation. Thereafter, the pristine configuration is recovered by back-electron transfer directly from the d_{z^2} state or indirectly from another d state (e.g., a $d_{xy} \rightarrow$ GS CT followed by a $d_{z^2} \rightarrow d_{xy}$ electron−hole recombination). The lifetime of the porphyrin ESA corresponds to the time of this back-donation. The remaining 14% undergoing internal conversion to the Q band (channel B) reach the same antibonding metal state through a less energetically favorable crossing point, triggering a delayed photodissociation. The more favorable path to d_{xy} (channel C) is prevented by the full occupancy of this state. The hypothesis of a phonon-assisted process to overcome the crossing point is corroborated by the shortening of the Q emission lifetime with the excitation energy (Table 1), and in Figure S5 this is represented by the height of crossing point with respect to the minimum of S_1.

In the ferric form, the most favorable relaxation pathway is open to the partially occupied d_π orbital, allowing a faster de-excitation without bond-cleavage (step 2, red arrow).[12] The lack of photodissociation upon excitation in the B band suggests that the hole on the d_π orbital can open a similar relaxation via the nonbonding state from S_2. Alternatively, the first electron transfer may still end up on the d_{z^2} orbital, but the presence of an empty hole on the lower d_π allows intrametal relaxation capable of depopulating the antibonding state before any bond-cleavage occurs (in Figure S5, it would correspond to the crossing point between the d_{z^2} and d_π surfaces). After 150−200 fs, the system reaches the same state, responsible for the ESA signal, regardless of the oxidation state and the excitation frequency.

CONCLUSIONS

Femtosecond-resolved fluorescence studies of Cyt *c* upon UV excitation have been carried out, revealing a subpicosecond energy transfer from the Trp to the haem, strongly dependent on the oxidation state of the latter. This result stresses the different geometries (distance and relative orientation) of the Trp−haem pair in ferrous and ferric Cyt *c*. We reported time-resolved ultrafast fluorescence from the photoexcited haem group, which reveals a complex multichannel electronic relaxation. The broad detection range as well as the excitation tunability of the transient fluorescence and absorption allowed us to follow the different relaxation steps and to propose that the photolysis in ferrous Cyt *c* is triggered by a charge transfer from the excited states of the porphyrin ring to the d_{z^2} antibonding orbital of the iron. This relaxation channel is <40 fs from S_2 or from upper energy levels, but 100−150 fs from S_1. The latter time constant strongly depends on the excess of vibrational energy, which is evidence of a phonon-assisted process to overcome an energy barrier before the charge transfer can occur. In the ferric form, the presence of the partially unoccupied d_π orbital constitutes a faster decay channel, which prevents the ligand from dissociating.

ASSOCIATED CONTENT

Supporting Information. Figures showing (i) the wavelength- and time-resolved fluorescence of Cyt *c*; (ii) transient absorption spectra at different delay times and the corresponding decay associated spectra (DAS); (iii) DAS of emission spectra and kinetic trace of fluorescence; (iv) emission spectra at 0 and 120 fs time delays; and (v) potential energy diagram of ferrous and ferric Cyt *c* haem, with proposed relaxation pathways. This material is available free of charge via the Internet at http://pubs.acs.org.

AUTHOR INFORMATION

Corresponding Author

*E-mail: majed.chergui@epfl.ch.

Present Addresses

† Institute of Applied Physics, University of Bern, Silderstrasse 5, CH-3012 Bern, Switzerland.

ACKNOWLEDGMENT

We thank Dr. Frank van Mourik for useful discussions. This work was partly supported by the Swiss NSF through the NCCR MUST-"Molecular Ultrafast Science and Technology".

REFERENCES

(1) Franzen, S.; Kiger, L.; Poyart, C.; Martin, J. L. *Biophys. J.* **2001**, *80*, 2372–2385.
(2) Kholodenko, Y.; Gooding, E. A.; Dou, Y.; Ikeda-Saito, M.; Hochstrasser, R. M. *Biochemistry* **1999**, *38*, 5918–5924.
(3) Lim, M.; Jackson, T. A.; Anfinrud, P. A. *Science* **1995**, *269*, 962–966.
(4) Hamada, D.; Kuroda, Y.; Kataoka, M.; Aimoto, S.; Yoshimura, T.; Goto, Y. *J. Mol. Biol.* **1996**, *256*, 172–186.
(5) Martin, J. L.; Vos, M. H. *Hemoglobins, Part C* **1994**, *232*, 416–430.
(6) Petrich, J. W.; Martin, J. L.; Houde, D.; Poyart, C.; Orszag, A. *Biochemistry* **1987**, *26*, 7914–7923.
(7) Petrich, J. W.; Poyart, C.; Martin, J. L. *Biochemistry* **1988**, *27*, 4049–4060.
(8) Steiger, B.; Baskin, J. S.; Anson, F. C.; Zewail, A. H. *Angew. Chem., Int. Ed.* **2000**, *39*, 257–+.
(9) Baskin, J. S.; Yu, H. Z.; Zewail, A. H. *J. Phys. Chem. A* **2002**, *106*, 9837–9844.
(10) Green, D. R.; Reed, J. C. *Science* **1998**, *281*, 1309–1312.
(11) Hengartner, M. O. *Nature* **2000**, *407*, 770–776.
(12) Negrerie, M.; Cianetti, S.; Vos, M. H.; Martin, J. L.; Kruglik, S. G. *J. Phys. Chem. B* **2006**, *110*, 12766–12781.

(13) Wang, W.; Ye, X.; Demidov, A. A.; Rosca, F.; Sjodin, T.; Cao, W. X.; Sheeran, M.; Champion, P. M. *J. Phys. Chem. B* **2000**, *104*, 10789–10801.
(14) Hochstrasser, R. M.; Negus, D. K. *Proc. Natl. Acad. Sci. U.S.A.* **1984**, *81*, 4399–4403.
(15) Janes, S. M.; Holtom, G.; Ascenzi, P.; Brunori, M.; Hochstrasser, R. M. *Biophys. J.* **1987**, *51*, 653–660.
(16) Yeh, S. R.; Han, S. W.; Rousseau, D. L. *Acc. Chem. Res.* **1998**, *31*, 727–736.
(17) Goto, Y.; Calciano, L. J.; Fink, A. L. *Proc. Natl. Acad. Sci. U.S.A.* **1990**, *87*, 573–577.
(18) Sanchez, K. M.; Schlamadinger, D. E.; Gable, J. E.; Kim, J. E. *J. Chem. Educ.* **2008**, *85*, 1253–1256.
(19) Qiu, W. H.; Li, T. P.; Zhang, L. Y.; Yang, Y.; Kao, Y. T.; Wang, L. J.; Zhong, D. P. *Chem. Phys.* **2008**, *350*, 154–164.
(20) Stevens, J. A.; Link, J. J.; Kao, Y. T.; Zang, C.; Wang, L. J.; Zhong, D. P. *J. Phys. Chem. B* **2010**, *114*, 1498–1505.
(21) Zhang, L. Y.; Kao, Y. T.; Qiu, W. H.; Wang, L. J.; Zhong, D. P. *J. Phys. Chem. B* **2006**, *110*, 18097–18103.
(22) Ha-Thi, M. H.; Shafizadeh, N.; Poisson, L.; Soep, B. *Phys. Chem. Chem. Phys.* **2010**, *12*, 14985–14993.
(23) Ishizaka, S.; Wada, T.; Kitamura, N. *Photochem. Photobiol. Sci.* **2009**, *8*, 562–566.
(24) Sorgues, S.; Poisson, L.; Raffael, K.; Krim, L.; Soep, B.; Shafizadeh, N. *J. Chem. Phys.* **2006**, *124*, 114302.
(25) Consani, C.; Bräm, O.; van Mourik, F.; Cannizzo, A.; Chergui, M. *Chem. Phys.* **2011**, doi: 10.1016/j.chemphys.2011.09.002.
(26) Henry, E. R.; Eaton, W. A.; Hochstrasser, R. M. *Proc. Natl. Acad. Sci. U.S.A.* **1986**, *83*, 8982–8986.
(27) Cannizzo, A.; Bram, O.; Zgrablic, G.; Tortschanoff, A.; Oskouei, A. A.; van Mourik, F.; Chergui, M. *Opt. Lett.* **2007**, *32*, 3555–3557.
(28) Bräm, O.; Cannizzo, A.; Oskouei, A. A.; Tortschanoff, A.; van Mourik, F.; Chergui, M. *Ultrafast Phenomena Xvi* **2009**, *92*, 346−348, 1031.
(29) Vengris, M.; van der Horst, M. A.; Zgrablic, G.; van Stokkum, I. H. M.; Haacke, S.; Chergui, M.; Hellingwerf, K. J.; van Grondelle, R.; Larsen, D. S. *Biophys. J.* **2004**, *87*, 1848–1857.
(30) Zgrablic, G.; Voitchovsky, K.; Kindermann, M.; Haacke, S.; Chergui, M. *Biophys. J.* **2005**, *88*, 2779–2788.
(31) Consani, C.; Prémont-Schwarz, M.; ElNahhas, A.; Bressler, Ch.; van Mourik, F.; Cannizzo, A.; Chergui, M. *Angew. Chem. Int. Ed.* **2009**, *48*, 7184–7187.
(32) Gouterman, M. *J. Mol. Spectrosc.* **1961**, *6*, 138–&.
(33) Butt, W. D.; Keilin, D. *Proc. R. Soc. London, Ser. B* **1962**, *156*, 429–&.
(34) Gouterman, M.; Snyder, L. C.; Wagniere, G. H. *J. Mol. Spectrosc.* **1963**, *11*, 108–&.
(35) Tsong, T. Y. *J. Biol. Chem.* **1974**, *249*, 1988–1990.
(36) Tsong, T. Y. *Biochemistry* **1976**, *15*, 5467–5473.
(37) Loewenich, D.; Kleinermanns, K. *Photochem. Photobiol.* **2007**, *83*, 1308–1312.
(38) Vivian, J. T.; Callis, P. R. *Biophys. J.* **2001**, *80*, 2093–2109.
(39) Bram, O.; Oskouei, A. A.; Tortschanoff, A.; van Mourik, F.; Madrid, M.; Echave, J.; Cannizzo, A.; Chergui, M. *J. Phys. Chem. A* **2010**, *114*, 9034–9042.
(40) Szabo, A. G.; Rayner, D. M. *J. Am. Chem. Soc.* **1980**, *102*, 554–563.
(41) Schweitzer-Stenner, R. *J. Phys. Chem. B* **2008**, *112*, 10358–10366.
(42) Schejter, A.; Plotkin, B. *Biochem. J.* **1988**, *255*, 353–356.
(43) Eden, D.; Matthew, J. B.; Rosa, J. J.; Richards, F. M. *Proc. Natl. Acad. Sci. U.S.A.* **1982**, *79*, 815–819.
(44) Steer, R. P.; Tripathy, U.; Kowalska, D.; Liu, X.; Velate, S. *J. Phys. Chem. A* **2008**, *112*, 5824–5833.
(45) Champion, P. M.; Lange, R. *J. Chem. Phys.* **1980**, *73*, 5947–5957.
(46) Champion, P. M.; Perreault, G. J. *J. Chem. Phys.* **1981**, *75*, 490–491.
(47) Liao, M. S.; Scheiner, S. *J. Chem. Phys.* **2002**, *116*, 3635–3645.
(48) Bräm, O.; Messina, F.; El-Zohry, A.; Cannizzo, A.; Chergui, M. *Chem. Phys.* **2011**submitted.